Cervical Intervertebral Motion as a Soft-Tissue Injury Predictor for Neck Hyperextension in Low-Speed Rear Impacts

Reed Finfrock, Alexander Bendig, Colton Thomas, William Millis, Kevin Moorhouse, Yun-Seok Kang

Abstract: Whiplash-associated disorders remain prevalent in low-speed rear impacts, yet current injury assessment frameworks rely predominantly on global neck metrics that lack the specificity to identify soft-tissue injury location. This study evaluates cervical intervertebral kinematics as segment-level predictors of soft-tissue injury during hyperextension in low-speed rear impacts. Six post-mortem human subjects (PMHS) were exposed to controlled low-speed rear-impact pulses ($\Delta V \approx 9$ km/h) using a simplified seat without a head restraint. Vertebral kinematics were captured using six-degree-of-freedom motion blocks at C2 through T1, and post-test dissection confirmed soft-tissue injury outcomes at intervertebral levels. All subjects exhibited pronounced retraction, S-shaped cervical curvature, hyperextension paired with substantial head-to-T1 relative rotation (HTTRR; 45–66°), followed by flexion rebound. Peak intervertebral extension ranged from 5–12°, with the largest rotations observed at C4–C5 and C6–C7. Intervertebral extension and the peak flexion to peak extension range were strongly associated with soft-tissue injury. Notably, normalised intervertebral extension emerged as the strongest predictor (AUROC = 0.91; GKG = 0.81; $p = 0.008$). Injury risk curves were developed based on these predictors. These findings support the integration of segment-level intervertebral metrics into cervical injury assessment frameworks as more anatomically specific alternatives to global neck criteria.

Keywords: Cervical Spine, Intervertebral Kinematics, Low-Speed Rear Impact, PMHS, Whiplash-associated disorders (WAD).

I. INTRODUCTION

Cervical injuries, even without fracture, frequently present themselves as chronic and debilitating conditions that negatively affect quality of life long after exposure to trauma [1]. Non-recovery rates are high, with over 50% of individuals reporting persistent symptoms for two years following clinical cervical trauma [1]. Prevention and management are further complicated because these injuries frequently arise in the absence of visually identifiable cervical spine abnormalities [2]. Following a motor vehicle crash, cervical injuries in absence of fracture are the most common injuries leading to permanent medical impairment [3]. Whiplash-associated disorders, including cervical spine injuries, remain common in low-speed rear impacts [4].

While there were increased efforts to reduce the whiplash-associated disorders, including head to T1 rearward rotation (HTTRR) limits in FMVSS No. 202a [5], NIC, Nkm, T1 acceleration, head acceleration, and head contact time in Euro NCAP [6], neck loads in JNCAP [7], and through T1 acceleration, Nkm, head contact time, and head–pelvis relative velocity in IIHS evaluations [8], most rear-impact tests remain largely focused on global neck injury potential. The heterogeneity of neck motion can localise potentially injurious kinematic or dynamic exposures to specific vulnerable segments. Though previous research demonstrated that increased neck loading is associated with increased vertebral loads [9-11], evaluating cervical kinematics by considering localised loading conditions throughout an event can more directly characterise the mechanisms pertinent to soft tissue injury. Component experiments of the isolated cervical spine have emphasised the role of intervertebral rotation on the physiological motion patterns of the cervical spine [11]. While cervical kinematics and intervertebral kinematics have been documented across a few experiments [12–14] specific thresholds have yet to be established for integration into neck injury protection strategies. Because localised loading directly drives non-physiological motion patterns that instigate injury [11], investigation into the detailed cervical kinematics offers deeper insight into the potential injury mechanisms than global metrics.

This study aims to characterise cervical vertebral and intervertebral kinematics during rear-impact hyperextension to evaluate if intervertebral level responses demonstrate stronger associations with soft-tissue

R. Finfrock is a PhD candidate (Finfrock.25@buckeyemail.osu.edu). Y. Kang is a professor in the Injury Biomechanics Research Center (IBRC) at The Ohio State University in Columbus, OH, USA. C. Thomas, W. Millis and K. Moorhouse are at the National Highway Traffic Safety Administration (NHTSA), in East Liberty, OH, USA. Alexander Bendig is research staff at the Transportation Research Center in East Liberty, OH, USA.

injury than conventional global neck metrics. Relationships between injury outcomes, intervertebral rotation, and extension-phase kinematics were examined by comparing these candidate metrics against existing neck injury criteria. Finally, using injury outcomes determined from dissections, injury risk curves for most predictive variables were developed to establish more sensitive, vertebral level injury predictors for the cervical spine.

To evaluate the utility of vertebral kinematics, multiple intervertebral kinematic parameters were treated as candidate injury predictors including peak intervertebral extension, the flexion-to-extension peak-to-peak range, rotation rates, and three normalization variants designed to reduce inter-subject and inter-segmental variability. These candidates were shown in tandem to conventional global neck injury criteria, such as HTTRR, NIC, and Nkm, to identify the parameters most strongly associated with soft-tissue injury outcomes confirmed at dissection.

II. METHODS

Six mid-size male post-mortem human subjects (PMHS) were exposed to controlled low-speed rear-impact pulses (ΔV = 8.8–9.0 km/h) to evaluate cervical spine kinematics during hyperextension.

General Sled Set-up

Figure 1 shows a general sled set-up. A specialised seat, designed without a head restraint and featuring a reduced seatback height, was incorporated into a mini-sled system to enable complete cervical extension [15]. The height of the seatback is adjusted to align the top with the T8 vertebra (Fig. 1A). The seatback top was rounded (outer diameter = 11.4 cm) to avoid force concentration at any edge during extension. This controlled setup enables a mechanistic investigation of how extension influences cervical kinematics and injury potential. The seatback and seat pan were fixed at 24° from vertical and 19° from horizontal, respectively (Fig. 1B & 1C). The mini-sled seat was mounted on a raised rail system and halted by a spring-damper stopper (Fig. 1D). The subject head was held in place using support cables (Fig. 1E) and cut upon probe contact with the energy transfer device (Fig. 1F) [16]. A support pole held the shoulder belt D-ring (Fig. 1G) for restraint tensioning (17.8 N lap, 26.7 N shoulder). Uniaxial accelerometers, (Endevco 7264C-2k, PCB Piezotronics, Inc., Halifax, NC, USA) were placed on the sled to capture the achieved pulse: one along the shoulder belt beam near the D-ring, one at the bottom of the beam, and one attached to the back of the seatback (Fig. 1H).

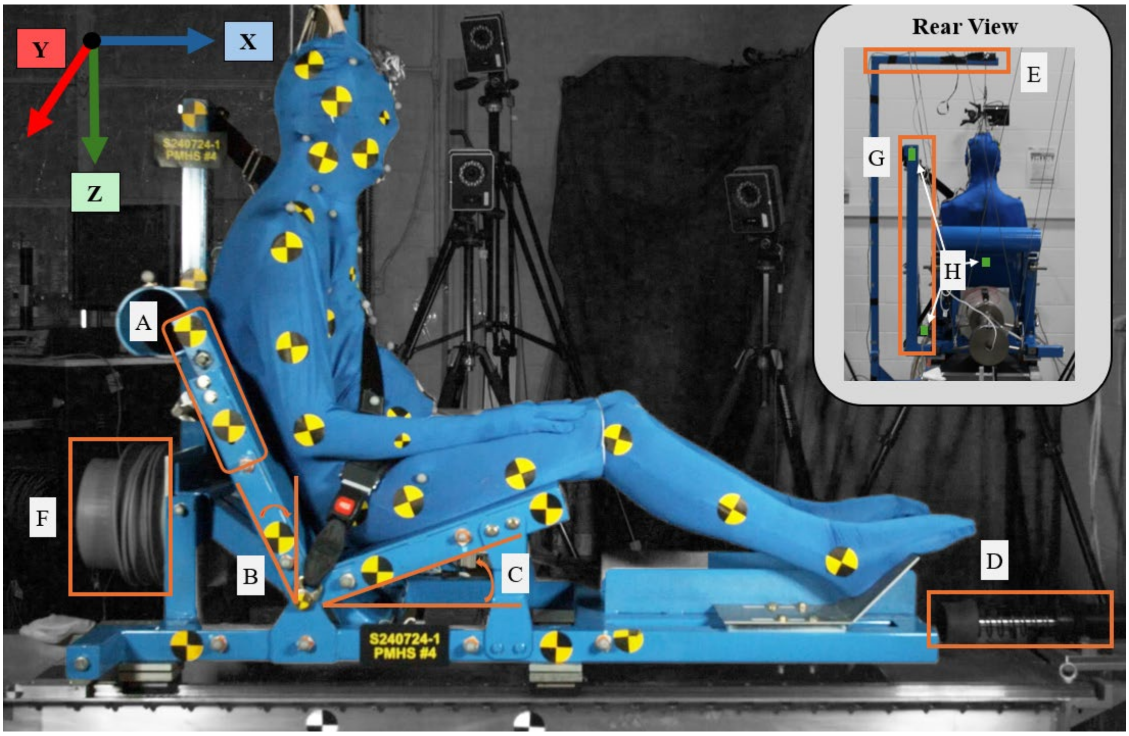

Fig. 1. Example Sled Test

PMHS Information

Detailed PMHS characteristics are provided in Table I. PMHS averaged 70 yrs old which is older than the 50th percentile male. PMHS were slightly taller and lighter than the 50th percentile male (Table I). PMHS were screened to confirm normal or osteopenia aBMD t-scores using dual-energy X-ray absorptiometry (DXA). PMHS were further screened through Computed Tomography (CT) scans, and PMHS with abnormal cervical spine conditions, such as pronounced cervical osteophytes or disc degeneration, were excluded.

TABLE I
PMHS INFORMATION

Subject	Age (yrs)	Height (cm)	Weight (kg)	aBMD T-Score L2-L4	Test Reference Number
PMHS1	61	176.6	60.1	-1.2	15792
PMHS2	81	171.8	67.0	0.0	15793
PMHS3	54	179.0	75.8	-2.4	15794
PMHS4	87	177.7	63.7	-1.9	15795
PMHS5	63	182.7	75.3	0.9	15796
PMHS6	71	192.0	76.7	1.0	15797
Mean (SD)	70 (13)	180.0 (6.9)	69.8 (7.1)	-0.6 (1.3)	-
50th Male [17]	45	175.3	77.3	-	-

PMHS Instrumentation

PMHS instrumentation used a series of six-degree of freedom (6DOF) (6DX Pro, Diversified Technical Systems, Inc., Seal Beach, CA, USA) sensor arrays to collect information required in defining PMHS response. In addition, head kinematics were collected utilising a 6aω tetrahedron assembly. The 6aω consists of six accelerometers (Endevco 7264C-2k, PCB Piezotronics, Inc., Halifax, NC, USA) and three angular rate sensors (DTS-ARSPRO-18K, Diversified Technical Systems, Inc., Seal Beach, CA, USA). The tetrahedron data was transformed to the head center of gravity, which was measured in post-dissections [18]. Head angular velocities about the y-axis were numerically integrated to calculate rotations. PMHS cervical spine (C2–C7) and T1 were instrumented with 6DOF motion blocks placed on each vertebral body [19]. In addition to cervical spine instrumentation, 6DOF blocks were placed at T4, T8, T12, S1, the iliac wing, and the sternum to capture overall spinal kinematics and describe torso and pelvic motion throughout the test. The orientation of the 6DOF blocks relative to the bodies of interest was defined using CT scans for transformation of the data from the block's-center to each anatomical origin and rotated according to the anatomical axes used in previous studies [20-21]. 10 Vicon cameras (Vantage 5, Vicon Motion Systems Ltd., Oxford, UK) were used to capture motions of both the sled and the PMHS throughout the test. Although collected for future analysis, Vicon position data and 6DOF instrumentation beyond the head and neck (C2-T1) were outside the scope of this study.

PMHS Positioning

PMHS were centered on the seat, with the pelvis pushed against the seatback. The head angle (Frankfort plane) was adjusted to 0 ± 2°, while the shoulders were leveled. Following initial positioning, leg and thigh angles were recorded and controlled for consistency. Occupant general anatomical landmarks and surface geometry of the PMHS and test environment were determined using a FARO arm digitiser and 3D scanner (FARO Technologies, AMETEK, Inc., Lake Mary, FL). Finally, X-ray imaging was used to document pelvis angles, visualise XZ-plane instrumentation, and record initial spinal curvature (Fig. 1).

Data Collection

Data were collected using a SLICE PRO data acquisition system (Diversified Technical Systems, Seal Beach, CA, USA) at a sampling rate of 20,000 Hz. All signals were filtered in accordance with SAE J211 standards [22].

High-speed video was recorded from the side profile depicted in Fig. 1. Two cameras (Miro LC321S, Phantom AMETEK Inc., Wayne, NJ, USA) recorded the general PMHS kinematics at 500 frames per second for the first three tests and 1000 frames per second for the last three, where one recorded a close-up of the head and neck, the other recorded an overview of the entire sled.

Post-test, head mass properties were evaluated for use in inverse dynamics. Head mass properties were collected utilising the isolated head post-dissection on a balance and moment table assembly to calculate the location of the center of gravity and moments of inertia about each anatomical axis [23-24].

Injury Assessment

Detailed post-test dissections were conducted to assess injuries from all body regions, while the primary focus was the cervical spine. Manual flexion, extension, and torsional motions were applied to the isolated ligamentous cervical spine at each intervertebral level to evaluate soft-tissue injuries and intervertebral instability. Intervertebral laxity was defined as an abnormal increase in mobility, frequently accompanied by visible tissue differences. Injury outcomes were compared to intervertebral kinematics obtained during testing to evaluate the predictive capability of vertebral kinematics for soft tissue injuries.

Data Analysis

To quantify cervical spine response, kinematics were categorised into two groups. The first characterises the neck as a global structure, defining motion through head and torso loading such as HTTRR. Because mass properties are collected and external forces do not act on the head during the test, inverse dynamics can be used to calculate the effective forces that the head experiences to achieve the measured linear and angular accelerations [25]. These also enable the computation of kinetic parameters such as Nkm.

The second group evaluates localised behavior by quantifying motion at individual cervical vertebrae or intervertebral segments. Intervertebral rotations were calculated as relative rotation of the superior vertebra with respect to the adjacent inferior vertebra (e.g., C2–C3). Following this convention, positive values indicate intervertebral extension (greater rearward rotation of the superior vertebra), while negative values denote intervertebral flexion. Evaluated parameters included intervertebral rotation peaks, the total rotation from flexion to extension, the peak rotation rates, and the peak of the product of rotation and rotation rate. Flexion to extension peak-to-peak was calculated as the total intervertebral rotation from the maximum flexion (negative peak) to the maximum extension (positive peak). Intervertebral rotation normalization approaches were employed, along with the unnormalised intervertebral rotations, as candidates for association with soft-tissue injury. For terms such as HTTRR, positive relative rotation would be considered neck extension while negative is neck flexion. To classify total HTTRR including both flexion and extension, absolute values of the corresponding phases are added to define total rotation angle. Rotation polarity is used solely to differentiate flexion and extension. All peak values are reported as absolute magnitudes; thus, flexion values correspond to the absolute magnitude of the originally negative relative rotation.

Intervertebral Normalisation

Because intervertebral rotation varies across cervical levels due to anatomical differences, absolute rotation magnitude alone may not reliably identify injurious segments. To further examine the capacity of intervertebral rotation to predict cervical soft-tissue injuries, two normalisation techniques were proposed: one designed to minimise inter-subject variance and another to reduce inter-segmental variance. Within inter-subject normalisation techniques, two approaches were considered to characterise dynamic ROM. Inter-subject normalisation was motivated by the inherent variability in cervical spine geometry, morphology, and baseline flexibility, which produce different dynamic ranges of motion (ROM). An intervertebral rotation that represents non-physiological motion in one subject may fall within the typical physiological range of a more flexible cervical spine. The first technique used the mean intervertebral rotation across all cervical segments within a PMHS as a normalising denominator, to determine irregularity relative to the PMHS without ROM dependence. This technique is described in Equation 1.

$$\frac{\text{Peak Flexion}_{l_0}^{\text{PMHS}_x} + \text{Peak Extension}_{l_0}^{\text{PMHS}_x}}{\frac{1}{\text{Length set } (L)} \sum_{l \in L} \left(\text{Peak Flexion}_{\text{PMHS}_x}(l) + \text{Peak Extension}_{\text{PMHS}_x}(l) \right)} Set\ Average_{all\ PMHS\&Levels} \quad \text{Eq. (1)}$$

where:

$$L = \{\text{C2C3,C3C4,C4C5,C5C6,C6C7,C7T1}\}$$
$$x = any\ particular\ PMHS$$
$$l_0 = any\ particular\ level$$

Equation 1 uses the average intervertebral rotation considering all intervertebral levels of a single PMHS to establish a PMHS-dependent reference as a denominator. Here, L denotes the set of all intervertebral levels from C2C3 to C7T1, while lowercase l without subscript denotes any individual level within that set, iterated over in the denominator sum. By calculating the ratio of each individual intervertebral rotation to this mean, this technique captures relative deviation from that PMHS's motion patterns. To ensure the results remain physically interpretable rather than purely dimensionless, these ratios were rescaled by the average to represent test-specific rotation magnitudes. The rescaled value represents the rotation that would be expected at that level if the targeted variations were removed, preserving the comparability with unnormalised intervertebral rotations. This normalisation technique is phase-dependent such that if the numerator evaluates extension phase, the denominator is similarly derived only from extension data. This method, however, was susceptible to bias when non-physiological intervertebral rotations (i.e., rotations that exceed the expected physiological range for a given cervical level, potentially indicative of structural compromise) at injured levels skewed the subject average.

To address this, a second approach utilised HTTRR as a gross, subject-specific flexibility parameter, which is inherently less sensitive to localised injuries. Additionally, a total HTTRR term was used, incorporating both the peak flexion and peak extension to represent the full dynamic range of head-to-T1 rotation throughout the impact event. This technique is described in Equation 2.

$$\frac{\text{Peak Flexion}_{l_0\ \text{PMHS}_x} + \text{Peak Extension}_{l_0\ \text{PMHS}_x}}{\left(\text{Peak HTTRR}_{\text{Flexion PMHS}_x} + \text{Peak HTTRR}_{\text{Extension PMHS}_x}\right)} (Avg\ Peak\ HTTRR_{Flexion} + Avg\ Peak\ HTTRR_{Extension})_{all\ PMHS} \quad \text{Eq. (2)}$$

where:

$$x = any\ particular\ PMHS$$
$$l_0 = any\ particular\ level$$

Equation 2 uses the subject-specific HTTRR to establish a PMHS-dependent denominator. This approach generates ratios for each observed intervertebral rotation, effectively normalising intervertebral rotations to the HTTRR, which represents overall head-neck movement. Similar to Equation 1, this technique rescales the dimensionless ratios by the average HTTRR to maintain physically representative magnitudes. The denominator remains phase-specific; for instance, extension-only numerators are paired with the extension-only HTTRR denominator. Because HTTRR is a global metric, it is inherently less sensitive to localised injury response. Consequently, HTTRR was considered the stronger inter-subject normalisation term, although both metrics were retained for comparative statistical analysis.

The objective was not to develop separate intervertebral injury criteria for each anatomical level. Instead, each intervertebral motion was treated as a generic intervertebral unit within a pooled dataset. To account for inherent physiological differences between levels, inter-segmental normalisation was applied. By normalising each segment's mean rotation to its own level-specific mean response, injury prediction was based on relative deviations from typical behavior rather than absolute magnitude. This normalisation technique is described in Equation 3.

$$\frac{\text{Peak Flexion}_{l_0}^{\text{PMHS}_x} + \text{Peak Extension}_{l_0}^{\text{PMHS}_x}}{\frac{1}{n}\sum_{i=1}^{n} \text{Peak Extension}_{l_0}^{\text{PMHS}_i}} Set\ Average_{all\ PMHS\&Levels} \quad \text{Eq. (3)}$$

Where:

where:

$$n = total\ number\ of\ PMHS$$
$$x = any\ particular\ PMHS$$
$$l_0 = any\ particular\ level$$

Equation 3 uses the average intervertebral rotation of a specific anatomical level (e.g., all C5-C6 segments) to establish a segment-dependent denominator. This approach generates ratios for every observed intervertebral rotation within that specific intervertebral space, capturing deviation from level-specific motion patterns. Similar to previous methods, these ratios were rescaled by the average to maintain physically representative magnitudes. In initial evaluations, the denominator was restricted to extension data, while the numerator varied based on specific parameter being analysed. Ultimately, these normalisation procedures, along with the unnormalised intervertebral kinematics, were comparatively evaluated for their capability of identifying cervical levels subjected to potentially injurious loading conditions.

To show the influence of the normalisation procedures, an example depicts how each strategy influences the comparability of intervertebral rotations. Figure A1 shows an example of the normalisation procedure on peak values and its influence on the distribution of intervertebral rotation. Figure A1a is the recorded intervertebral rotation. Figure A1b is the normalised intervertebral rotation, such that the average value for PMHS intervertebral rotation is representative of the entire set of PMHS. Figure A1c is the normalised intervertebral rotation, such that the average value for segmental intervertebral rotation is representative of any intervertebral space. Figure A1d is the combined normalisation approach. Together these normalisation techniques depict how the normalisation procedure makes relative values more comparable and in what ways.

Statistical Analysis

To assess predictive capacity of each parameter for injury, binary logistic regression calculations were conducted using Minitab version 22 (Minitab LLC, Centre County, PA, USA). The analysis included calculations of Goodman-Kruskal Gamma (GKG) scores and the area under the receiver operating characteristic curve (AUROC), with significance determined by associated p-values. Injury risk curves were subsequently generated for the parameters demonstrating strong predictive capability. Mixed-effects binary logistic regression was considered to account for subject-specific clustering; however, with only six subjects, inter-subject variance could not be estimated reliably to characterize anatomical variability, and pooled logistic regression was retained as the primary analysis. To avoid imposing assumptions regarding the underlying distribution, Weibull, lognormal, and loglogistic parametric distributions were fitted alongside binary logistic regression. The mean estimate and confidence intervals for each method were plotted in conjunction with the nonparametric, consistent threshold method [26] to illustrate the sensitivity of injury risk to different distribution models. Finally, the normalisation techniques were evaluated to determine if isolating intervertebral responses from subject- and segment-specific variability improved the discrimination between injured and non-injured segments.

III. RESULTS

PMHS General Kinematics

Figure 2 shows the postural progression of the testing series at the listed sequence shown through images captured from high-speed video. The kinematic response followed a characteristic sequence: spinal straightening, initial neck retraction (often manifesting as pronounced S-shaped cervical curvature), followed by hyperextension, and concluding with a flexion rebound as inertial loading continues and the sled comes to a stop.

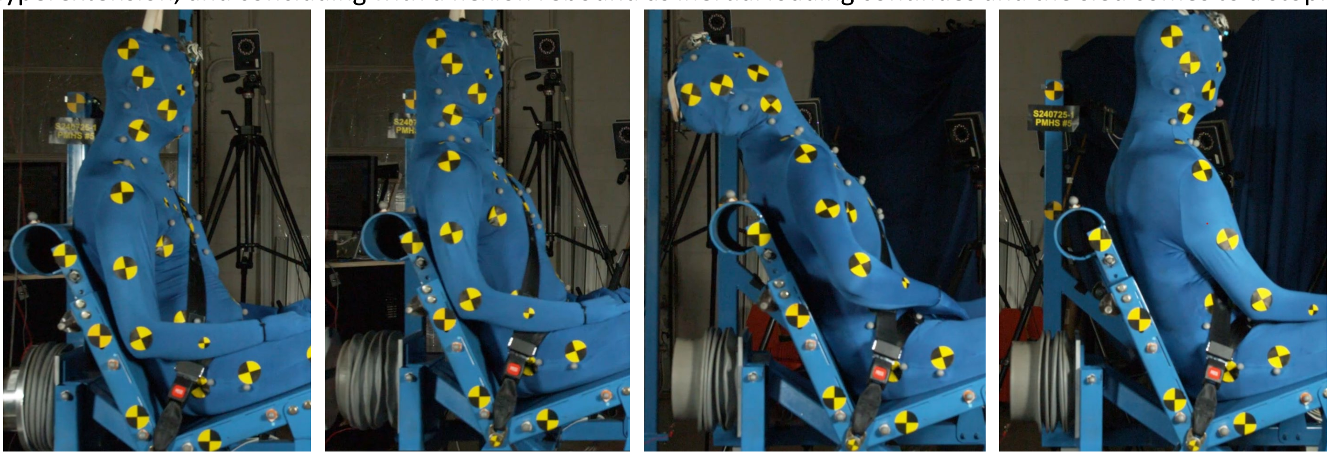

a) Initial posture b) Neck retraction c) Hyperextension d) Flexion rebound

Fig. 2: Sequential motion phases

Injury

Injury outcomes and cervical kinematic responses for all six PMHS are reported below. Table II shows the soft-tissue injuries for each test. All observed injuries were ligamentous laxity aside from PMHS 4, which had a partial tear of the anterior longitudinal ligament (ALL).

TABLE II
INJURY OUTCOMES

	Injuries
PMHS1	C4-C5 Laxity, C5-C6 Laxity
PMHS2	C4-C5 Laxity, C5-C6 Laxity, C6-C7 Laxity
PMHS3	No Injuries
PMHS4	C6-C7 Partial ALL Tear
PMHS5	C3-C4 Laxity, C6-C7 Laxity
PMHS6	C6-C7 Laxity

Existing Neck Injury Metrics

Table III shows the peak values for primary responses of HTTRR, force in x & z, moment in y, NIC and Nkm alongside injury results per PMHS. Peaks were selected from the time histories up to approximately 400 ms, which was after peak neck extension. General flexion and extension phases were defined through HTTRR polarity. HTTRR positive peaks were fairly consistent across subjects (45–54°) except PMHS6 which was notably higher (66°). HTTRR negative peaks are similarly consistent except PMHS4 which is nearly zero. Forces and moments show more variability but no clean separation between injured and uninjured. PMHS3 is the only uninjured subject yet has among the highest z direction force values and mid-range HTTRR. NIC and Nkm were elevated across all subjects with no apparent threshold distinguishing injured from uninjured cases. Additional peak values for whole neck metrics are shown in Table A1, where negative peaks of HTTRR are listed in addition to the opposite polarities for forces and moments shown in Table III.

TABLE III
WHOLE-NECK PARAMETERS

	HTTRR (+) °	**Force x (+)** N	**Force z (-)** N	**Moment y (-)** Nm	**NIC** m^2/s^2	**Nkm**	**# of Injuries**
PMHS1	49	188	-257	-15.5	18.2	0.47-NFP	2
PMHS2	45.2	147	-223	-10.9	12.6	0.36-NEP	3
PMHS3	48	189	-380	-12.2	17.5	0.37-NEP	0
PMHS4	47.6	190	-395	-8.4	15.4	0.40-NEP	1
PMHS5	54.4	188	-303	-10.4	26.2	0.38-NEP	2
PMHS6	66.4	152	-249	-14.1	19.6	0.45-NEP	1

Intervertebral Kinematics

To evaluate injury with respect to relative motion of the vertebrae, intervertebral rotation data is presented in Fig. 3. Across subjects, elevated intervertebral rotations were generally associated with increased injury occurrence. For example, PMHS 5 sustained injury at C6–C7, which exhibited higher intervertebral rotation than the uninjured C5–C6 segment within the same subject. Segmental kinematics are considered alongside kinematic phase by distinguishing HTTRR polarity. As shown in Fig. 2, retraction occurred first for all PMHS, followed by gross neck extension. PMHS 4 did not exhibit a retraction phase, rotating immediately into extension relative to T1.

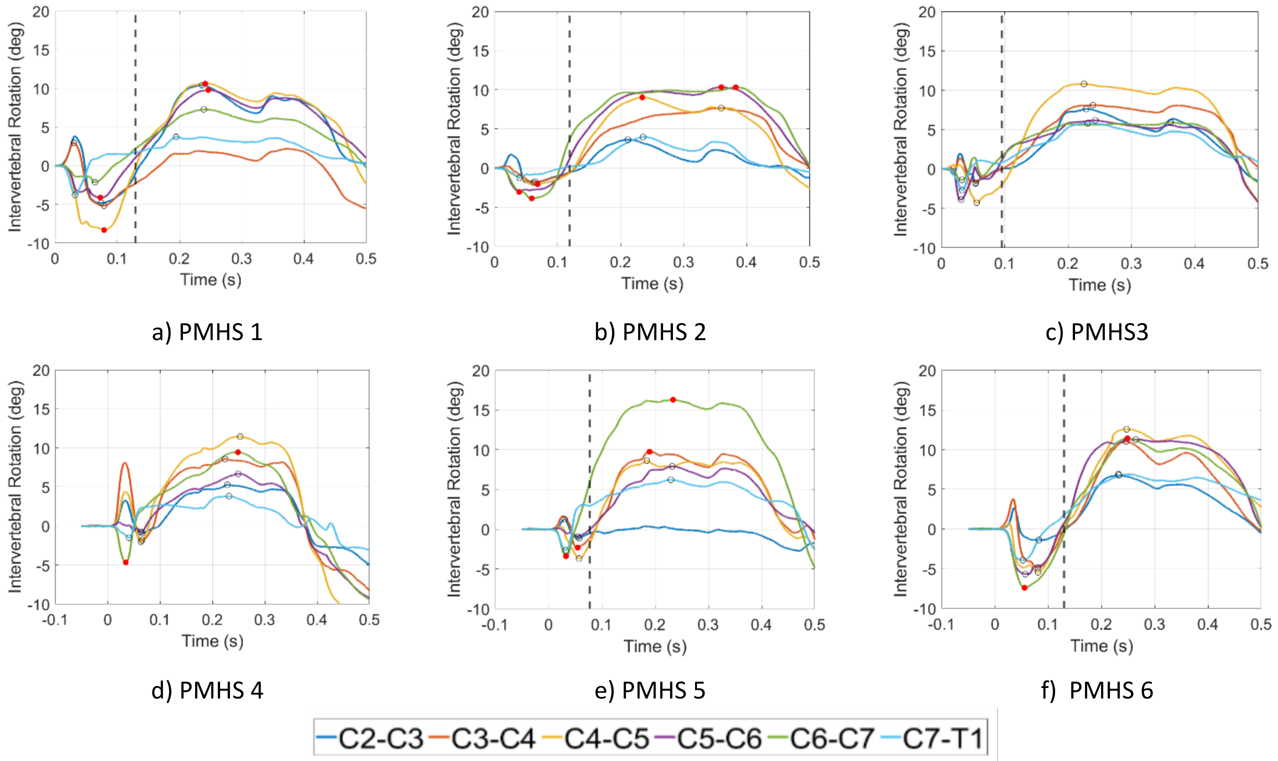

a) PMHS 1 b) PMHS 2 c) PMHS3

d) PMHS 4 e) PMHS 5 f) PMHS 6

Fig. 3: Intervertebral rotation time histories for each PMHS with injury outcomes. The circles represent the peak rotations at each level, with black open circles representing peaks where no injury observed and red filled circles represent peaks associated with injuries observed during post-test dissection. The black dashed vertical line marks the transition from retraction to extension phase, determined from HTTRR polarity.

Tables IV and V present the maximum intervertebral extension and flexion to extension peak-to-peak values, respectively, alongside subject and segment averages used for normalisation. Both tables show consistent trends: PMHS6 had the highest subject average of 10.0° extension and 14.7° flexion to extension peak-to-peak, compared to the set averages of 8.0° and 11.2°. Overall, peak intervertebral extension ranged from approximately 5–12° across cervical levels (Table IV). While intervertebral flexion to extension peak-to-peak typically ranged from 6-19° across cervical levels (Table V). The largest intervertebral rotations were commonly observed at C4–C5 and C6–C7 (Table IV & Figure 3). In contrast, upper and lower boundary segments (C2–C3 and C7–T1) generally exhibited smaller rotations.

TABLE IV

DYNAMIC MAX RELATIVE EXTENSION & NORMALISATION VALUES FOR EXTENSION (°)

	PMHS1	PMHS2	PMHS3	PMHS4	PMHS5	PMHS6		AVG Segment
C2-C3	10.4	3.6	7.6	5.3	1.2	6.8		**5.8**
C3-C4	2.2	7.7	8.1	8.6	9.8*	11.0		**7.9**
C4-C5	10.6*	9.0*	10.8	11.5	8.6	12.6		**10.5**
C5-C6	9.8*	10.3*	6.2	6.7	7.9	11.3		**8.7**
C6-C7	7.3	10.3*	5.9	9.4*	16.3*	11.4*		**10.1**
C7-T1	3.7	4.0	5.8	3.8	6.2	6.9		**5.1**
							Set Average	**8.0**
AVG PMHS	**7.3**	**7.5**	**7.4**	**7.5**	**8.3**	**10.0**	**8.0**	

*denotes injured levels

TABLE V
FLEXION TO EXTENSION PEAK TO PEAK & NORMALISATION VALUES (°)

	PMHS1	**PMHS2**	**PMHS3**	**PMHS4**	**PMHS5**	**PMHS6**		**AVG Segment**
C2-C3	15.2	5.5	9.4	6.2	2.4	8.2		**7.8**
C3-C4	8.1	9.4	9.9	10.4	12.1*	15.9		**10.9**
C4-C5	18.9*	11.1*	15.1	13.5	12.3	18.0		**14.8**
C5-C6	13.9*	13.4*	10.1	7.4	8.8	16.9		**11.8**
C6-C7	9.4	14.2*	7.3	14.1*	19.7*	18.8*		**13.9**
C7-T1	7.5	5.2	8.5	5.3	8.9	10.8		**7.7**
							Set Average	**11.2**
AVG PMHS	**12.2**	**9.8**	**10.0**	**9.5**	**10.7**	**14.8**	**11.2**	

*denotes injured levels

Statistics

Table VI shows the statistical outcomes for the binary regressions for each parameter. Intervertebral extension normalised by HTTRR peak showed the strongest performance, with an AUROC of 0.91, a GKG of 0.81, and a p-value of 0.008. The top eight parameters all achieved AUROC values above 0.8 and statistically significant p-values, with six of eight normalised flexion to-extension peak-to-peak metrics performing comparably to two of eight normalised extension-only metrics. Rotation-rate-based parameters and angular-rate-rotation products performed poorly, with AUROC values near 0.54–0.70 and non-significant p-values, suggesting limited discriminative capacity for injury prediction at the segmental level.

TABLE VI
STATISTICAL RESULTS PER SEGMENT

Variables	AUROC	GKG	P-Value
Intervertebral Extension Normalised by HTTRR Peak (Eq. 2)	0.91	0.81	0.008
Flexion to Extension Peak-to-Peak Normalised by PMHS Avg (Eq. 1)	0.90	0.80	0.006
Intervertebral Extension Normalised by PMHS Avg (Eq. 1)	0.89	0.78	0.010
Flexion to Extension Peak-to-Peak Normalised by Total HTTRR Peaks (Eq. 2)	0.88	0.75	0.007
Flexion to Extension Peak-to-Peak Relative Rotation	0.86	0.71	0.006
Flexion to Extension Peak-to-Peak Normalised by Segment Avg (Eq. 3)	0.86	0.71	0.006
Flexion to Extension Peak-to-Peak Normalised by HTTRR Peak (Eq. 2)	0.85	0.70	0.021
Intervertebral Extension	0.82	0.65	0.014
Product (Angular Rate * Rotation) Extension	0.70	0.39	0.499
Product (Angular Rate * Rotation) Flexion	0.69	0.38	0.486
Intervertebral Flexion	0.66	0.33	0.251
Intervertebral Extension Rotation Rates	0.54	0.09	0.617
Intervertebral Flexion Rotation Rates	0.53	0.05	0.627

Figure 4 presents injury risk curves for intervertebral extension, intervertebral extension normalised by HTTRR, and flexion to extension peak-to-peak normalised by PMHS average. Across all three, the plotted parametric distributions (Weibull, lognormal, loglogistic) and binary logistic regression produced closely agreeing curves. The Weibull distribution failed to converge for intervertebral extension. For intervertebral extension (Fig. 4a), the 50% injury risk threshold occurred at approximately 9°, though confidence intervals were wider, particularly in the upper tail. Extension normalised by HTTRR (Fig. 4b) produced relatively tight confidence intervals and strong agreement across all fitting methods, with a 50% risk threshold of approximately 10–11°, but parametric fits diverged somewhat from the consistent threshold method. The flexion to extension peak-to-peak curve (Fig. 4c) showed a higher 50% risk threshold of approximately 14–15°, with relatively tight confidence intervals and agreement across all methods including the consistent threshold method.

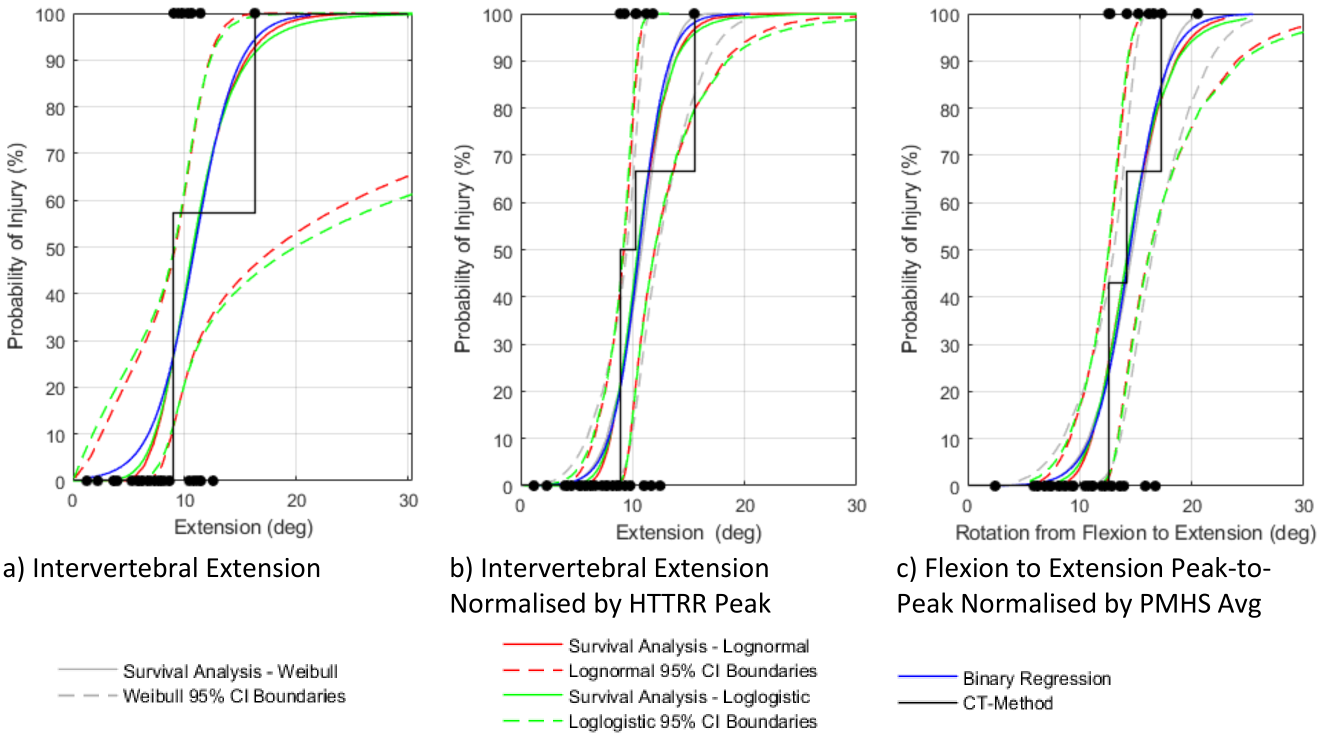

a) Intervertebral Extension

b) Intervertebral Extension Normalised by HTTRR Peak

c) Flexion to Extension Peak-to-Peak Normalised by PMHS Avg

Fig. 4: Injury risk curves for intervertebral extension, intervertebral extension normalised by HTTRR, and flexion to extension peak-to-peak normalised by PMHS average.

IV. DISCUSSION

Conventional neck injury criteria aggregate whole-neck response, potentially obscuring the segment-level conditions that underlie soft-tissue injury. This study examined whether intervertebral kinematics during rear-impact hyperextension associate more strongly with cervical injury than conventional global metrics. The results from this study demonstrate that intervertebral rotation and extension-phase kinematics provide superior associations with injury outcomes, in contrast, global metrics lacked the resolution to identify the specific vulnerable segments. These findings support the development of more sensitive, segment-level injury risk functions. The following discussion addresses the distribution of intervertebral rotation across cervical levels, the comparative performance of segmental to global injury criteria, and the derivation of injury risk functions from segment-level predictors.

PMHS General Kinematics

The PMHS response was grouped into distinct events following phases described in prior rear-impact studies [13], [27]: initial position, spinal straightening at impact, neck retraction, peak extension, and rebound. Different injury mechanisms have been linked to different phases of the response [27-29]. The initial response, during spinal compression and neck retraction, is the primary driver of the NIC criteria, theoretically causing spinal pressure changes that induce injury [28]. Following this, the hyperextension phase is the fundamental response governing non-physiological motion injury mechanisms [9], [11]. Nkm spans across the phases of motion, with components governed by the combination of force and moments within the neck [29]. In this study, PMHS 4 did not have a significant initial forward HTTRR, bypassing this relative flexion and moving straight into extension. This may be attributable to anatomical variation in resting cervical curvature. Prior modeling work has demonstrated that variation in initial cervical spine curvature influences response characteristics [30]. PMHS 4 exhibited comparatively greater lordotic curvature; however, quantitative analysis relating spine curvature to inertial interaction between the head and neck was left for future work.

Injury

Injuries occurred along the mid-to-lower cervical spine. These trends are similar to results on isolated ROM studies that found increased injury incidence at C5-C6 and C6-C7 [11]. All injuries in the cervical spine were identified as ligamentous laxity, except for a partial ALL tear at C6-C7 in PMHS 4. This PMHS exhibited the lowest whole-neck range of motion as measured by HTTRR, suggesting a globally stiffer cervical spine relative to other subjects. Despite this, intervertebral rotation at C6–C7 remained comparatively elevated, indicating that restricted global mobility may cause concentrated rotational demand at specific intervertebral segments. This localised loading concentration at C6–C7, in the context of reduced whole-neck motion, may have contributed to the more severe injury observed at that level, and illustrates a scenario in which whole-neck metrics would underestimate segment-level injury risk. These trends are shown in Fig. 5, which contrasts average uninjured intervertebral rotations with those observed at the injured regions.

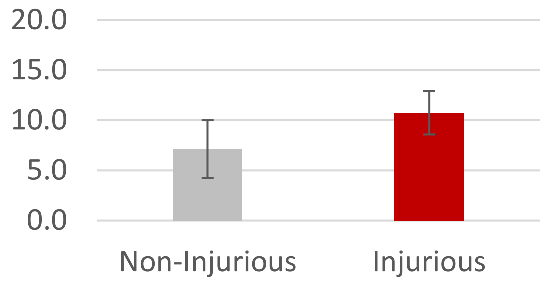

a) Extension Average Values

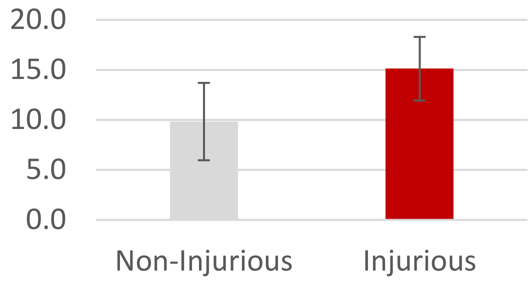

b) Flexion to Extension Average Values

Fig. 5: Non-Injured vs Injured Average Values

Existing Neck Injury Metrics

Comparison of the current findings with traditional global injury metrics, such as HTTRR, NIC, and Nkm, proved challenging. These metrics are established through the gross kinematics of the neck and are designed to estimate injury potential for the neck as a whole. HTTRR averaged 51.8° with a range from 45-66°. While these values greatly exceed the 12° posterior head-to-torso angular rotation limit that head restraints must provide under FMVSS 202a [5], these values are comparable to previous rear impact testing without a head restraint with values reported ranging from 40-70° across tests [12-13], [31]. It should be noted that this threshold was established for evaluating head restraint performance with the Hybrid III dummy and is not directly applicable to PMHS, other dummies, or to the no head restraint condition tested in the current study. Notably, PMHS 3 exhibited 48 degrees of extension without injury (Table IV). Furthermore, all PMHS exceeded the NIC threshold of 15 m^2/s^2 and five of six exceeded the Nkm threshold of 0.35, both of which were previously established as the lower performance threshold in Euro NCAP low severity protocols [6], [32]. Across tests, PMHS 3 exhibited maximum or near-maximum forces despite sustaining no injuries, while the associated moments remained close to the sample mean. While these criteria collectively indicate potential for injury across the test series, the criteria offer no mechanism for identifying specific vulnerable vertebral levels, the extent of segment involvement, or whether magnitudes that more substantially exceed established thresholds correspond to greater injury frequency or severity. Consequently, while global metrics may serve as valuable indicators of overall cervical injury risk, they are fundamentally limited in predicting injury location or the distribution of damage, an essential gap that intervertebral kinematic parameters are better positioned to address.

Global Hyperextension vs Local Criteria Development

The experimental design intentionally removed the head restraint to enable controlled and complete hyperextension, establishing conditions necessary to characterize the relationship between segment-level kinematics and soft-tissue injury. It is acknowledged that modern head restraint designs have reduced the prevalence of gross hyperextension in real-world rear impacts. Where gross hyperextension does occur, through occupant ramping or head restraint misuse, injury outcomes are governed by conditions near the specific injury rather than gross head-neck kinematics. While head restraint use maintains protective value by limiting gross cervical extension, segment-level criteria governing soft-tissue injury onset remain underdefined for use in head restraint performance standards. Excessive intervertebral rotation reduces the spine's ability to maintain stable intervertebral motion, disturbing pain-sensitive structures including those protected by facet capsule ligaments and the dorsal root ganglion through excursions beyond normal motion limits [11], [27]. Characterizing the relationship between excessive rearward intervertebral rotation and soft-tissue condition provides a step toward segment-level injury criteria, which may inform refinement of head restraint performance standards or evaluation of conditions where intervertebral rotation governs injury risk.

Intervertebral Kinematics

Prior anthropomorphic test device (ATD) studies compared extension behavior between the Hybrid III and BioRID to examine the effects of backset, the distance from head to the head restraint, on HTTRR [15]. Even with an excessive backset, PMHS from the previous study did not show intervertebral extension in the lower cervical segments [16]. This lack of intervertebral extension prevented the evaluation of criteria relating intervertebral extension to injury potential. These limitations informed the design of the current experimental seat, which removed the head restraint, to enable inverse dynamics calculations without head contact and lowered the seatback to facilitate complete cervical extension at each intervertebral level. This configuration allowed for the development of segment-level injury criteria.

In contrast to the lack of clear segmental trends reported in previous studies [12-13], [31] the current results suggest that mid-to-lower cervical segments bear a disproportionate rotational demand during rear-impact hyperextension. This pattern is consistent with head-neck evaluations which found similar increased rotation of the mid-to-lower segments [33]. Segments adjacent to the head and thorax, C2–C3 and C7–T1, showed reduced relative motion, likely reflecting the constraining inertial influence of those larger adjacent masses. While average intervertebral rotations were broadly consistent with prior PMHS low-speed rear-impact studies [12-13],[31] (8.11° vs. 10.3°, 7.1°, and 5.9°, respectively), notable heterogeneity at specific levels was observed. The implications of this variation differ by application. For the development of ATD injury assessment reference values or a generalisable intervertebral injury criteria, standardizing response across segments may be appropriate. However, for level-specific evaluation, this variation likely reflects genuine segment-level biomechanical differences and should not be normalised across levels. Intervertebral rotations that deviated from typical motion patterns corresponded to increased instances of soft-tissue injury, suggesting that localised, disproportionate motion may serve as a meaningful indicator of structural compromise.

Statistic Outcomes

To identify the most predictive kinematic to soft-tissue injury, multiple intervertebral rotation parameters were evaluated. Intervertebral rotation rate, the product of intervertebral rotation and rotation rate, and intervertebral flexion did not achieve statistical significance (Table VI). Among the evaluated parameters, intervertebral extension and the flexion to extension peak-to-peak range both achieved significance ($\alpha = 0.05$). Normalisation techniques derived from these two metrics also demonstrated statistical significance, with flexion to extension peak-to-peak values providing better statistical support. Normalisation generally improved statistical outcomes; the most predictive results were achieved by normalising extension using PMHS-specific HTTRR extension (AUROC = 0.91; GKG = 0.81; $p = 0.008$ in Table VI). Incorporating the flexion peak to characterise the full dynamic rotational range also improved predictive capacity; the flexion to extension peak-to-peak metric (AUROC = 0.86; GKG = 0.71; $p = 0.006$) outperformed intervertebral extension alone (AUROC = 0.82; GKG = 0.65; $p = 0.014$). These results suggest that accounting for subject-level range of motion variance more precisely isolates the rotational deviations associated with soft-tissue injury. Notably, each parameter independently demonstrated strong predictive capability, suggesting that absolute intervertebral rotation remains a meaningful indicator even without normalisation. Consequently, while the normalised extension curve (Fig. 4b) yielded the strongest statistical performance, unnormalised intervertebral rotation was also provided to examine independent of response-based normalisation. The marginal improvement observed when normalising the flexion to extension peak-to-peak metric by both the flexion and extension components may suggest that total HTTRR range does not fully capture the relevant dynamics limits. Therefore, predictive performance of this parameter may further improve with a more refined normalisation parameter.

Implementation

The ability to detect any injury potential may be sufficient in a surrogate context, as protective criteria primarily serve to guard against the initial injurious event rather than predict the distribution of injuries across multiple segments. Figure A2 demonstrates that HTTRR correlated with mean segmental extension response at the vertebral level, suggesting that intervertebral rotation scales predictably with gross neck motion. This relationship reinforces the theoretical basis for HTTRR as a global injury indicator while providing a localised kinematic foundation that links the gross head-to-T1 response to the segmental mechanics governing soft-tissue loading. Conversely, Fig. A3 and A4 illustrate that NIC and Nkm are not directly correlated with extension values. Figures A5 and A6 show the time histories of Nkm (Figure A5a), Nkm-NEP component (Figure A5b), and NIC injury criteria values (Fig. A6). It is logical that certain Nkm extrema may relate to intervertebral rotations, specifically when Nkm values are driven by extension (NEA & NEP). However, Nkm is a multi-component metric, and its peak values are not always dominated by extension. NIC peaks, on the other hand, occur during the initial retraction phase and consequently do not correlate with the maximum extension values observed later during the tests. Intervertebral rotation may therefore serve as a more direct, localized indicator of hyperextension injury potential. Theoretically, a relationship between HTTRR and cervical extension could then map intervertebral rotations approaching injurious thresholds to corresponding values of HTTRR or similar global metrics in standard seating configurations. Developing such a mapping requires further investigation into the relationship between HTTRR and intervertebral rotation in low-speed rear impacts involving head restraint contact. In these scenarios, gross neck motion is attenuated, yet segmental loading patterns may still reach critical thresholds at specific vertebral levels.

Limitations

Several limitations inherent to the study design warrant consideration. The sample size of six PMHS, while consistent with the practical constraints of PMHS biomechanics research, restricts the statistical power of the findings and the generalisation of the derived injury risk curves. To increase the effective sample size, observations were pooled across cervical levels, treating each intervertebral segment as an independent observation, similar to the approach applied when evaluating flexion [34]. This approach, however, involves the simplifying assumption that cervical segments are anatomically comparable and independent, despite known variation in geometry along the cervical spine and influence of adjacent levels. Intra-subject pooling is nonetheless defensible: intervertebral rotation is a relative motion metric whose value at a given intervertebral level reflects the coupled response of the cervical spine, and measures drawn from the same spine provide normalization context that cross-subject independent observations would not. Injury at one level likely absorbs a portion of the energy input, reducing loading at adjacent levels, and observations from those levels remain valid indicators that the recorded kinematics did not produce injury. This mechanism may have contributed to a natural mix of injurious and non-injurious observations across levels within the same specimen, a structure appropriate for a generalized injury criterion. Injury risk curves were fit treating all level-observations as independent, which is acknowledged as a preliminary approach; were additional data available, injurious observations would likely be less clustered within subjects and the resulting curves might show wider variance.

Injury also inflates the normalisation metric, which motivated the use of HTTRR to quantify subject physiological ROM. In addition, PMHS are unable to replicate active muscular response, which influences occupant kinematics in aware occupants; however, the passive muscular state of PMHS approximates the response of an occupant with no advanced awareness of an impending collision [35 - 36]. Pain perception represents an additional inherent limitation, as soft-tissue injury cannot be identified through symptom reporting in PMHS testing. Consequently, injury classification relies on the established relationship between non-physiological increases in intervertebral ROM and post-injury ligamentous laxity identified through dissection. This methodology is dependent on the validity of an associative framework that suggests that clinical pain is affiliated with non-physiological increases in ROM that present themselves after injury. However, these limitations are offset by the ability to evaluate cervical spine response to loading conditions that cannot be replicated in volunteer testing without significant risk of injury.

V. CONCLUSION

This study provides a novel, full-body PMHS dataset that directly links dynamic cervical intervertebral kinematics to soft-tissue injury outcomes during low-speed rear impacts. Intervertebral extension, along with the flexion to extension peak-to-peak range and its normalised derivatives, demonstrated statistically significant associations with soft-tissue injury. These findings support the integration of segment-level kinematic metrics into injury assessment frameworks as more sensitive, anatomically specific alternatives to traditional global neck criteria. The injury risk curves developed in the current study provide probabilistic soft-tissue injury thresholds across multiple statistical methods, offering a quantitative basis for evaluating cervical injury risk at intervertebral levels. Furthermore, the established correlation between HTTRR and mean segmental extension response could offer a practical means for interpreting ATD HTTRR limits. This relationship enables global kinematics to be contextualised as proxies for underlying segmental responses, even in surrogate testing configurations where direct intervertebral measurement is not feasible. Collectively, these findings advance cervical injury biomechanics toward segment-specific injury criteria that more accurately reflect the localised loading conditions governing non-physiological intervertebral motion and the ligamentous damage.

VI. ACKNOWLEDGEMENTS

We would like to start by thanking the anatomical donors, whose generous gift made this research possible. In addition, we would like to thank Angelo Marcallini, Rosalie Connell, Timothy Wensink and all IBRC members of The Ohio State University (Columbus, OH, USA) for their contributions toward this research and support throughout testing. This research was supported by the National Highway Traffic Safety Administration under Contract No. 693JJ918D000019, Task Order No. 693JJ919F000063.

VII. REFERENCES

[1] Rydman, E., Ponzer, S., Brisson, R., Ottosson, C. and Pettersson-Järnbert, H. (2018) Long-term follow-up of whiplash injuries reported to insurance companies: a cohort study on patient-reported outcomes and impact of financial compensation. European Spine Journal, **27**(6): pp.1255–1261.

[2] Yeo, C. G., Jeon, I. and Kim, S. W. (2015) Delayed or missed diagnosis of cervical instability after traumatic injury: usefulness of dynamic flexion and extension radiographs. Korean J. Spine, **12**(3): p.146-149.

[3] Gustafsson, M., Stigson, H., Krafft, M. and Kullgren, A. (2015) Risk of permanent medical impairment (RPMI) in car crashes correlated to age and gender. Traffic Inj. geneprev., **16**(4): pp.353–361.

[4] Freeman, M. D. and Leith, W. M. (2020) Estimating the number of traffic crash-related cervical spine injuries in the United States; an analysis and comparison of national crash and hospital data. Accid. Anal. Prev., **142:**105571.

[5] National Highway Traffic Safety Administration (2025). Federal Motor Vehicle Safety Standard No. 202a: Head Restraints.

[6] Euro NCAP (2025) Crash Protection Rear Impact Protocol.

[7] National Agency for Automotive Safety and Victims' Aid. "Test Procedures and Evaluation Methods for Collision Safety Performance Tests (Front, Side and Rear)", https://www.nasva.go.jp/mamoru/en/assessment_car/crackup_test.html. [cited 2026 Mar. 15]

[8] The Insurance Institute for Highway Safety (2025) Whiplash Prevention Evaluation Rating Guidelines Version I.

[9] Ivancic, P. C., Panjabi, M. M. and Ito, S. (2006) Cervical spine loads and intervertebral motions during whiplash. Traffic Inj. Prev., **7**(4): pp.389–399.

[10] Ito, S., Ivancic, P. C., Panjabi, M. M., Cunningham, B. W. and Re, B. (2004) Soft tissue injury threshold during simulated whiplash: a biomechanical investigation. Spine (Phila. Pa. 1976)., **29**(9): pp.979–987.

[11] Panjabi, M. M., Nibu, K. and Choelewieki, J. (1998) Whiplash injuries and the potential for mechanical instability. European Spine Journal, **7**: pp.484–492.

[12] Sato, F., Nakajima, T., Ono, K., Svensson, M. Y. and Brolin, K. (2014) Dynamic cervical vertebral motion of female and male volunteers and analysis of its interaction with head/neck/torso behavior during low-speed rear impact. Proceedings of IRCOBI Conference, 2014, Berlin, Germany.

[13] Deng, B., Begeman, P. C., Yang, K. H., Tashman, S. and King, A. I. (2000) Kinematics of human cadaver cervical spine during low speed rear-end impacts. Stapp Car Crash Journal, **44**: pp.171–188.

[14] Ono, K., Kaneoka, K., Wittek, A. and Kajzer, J. (1997) Cervical injury mechanism based on the analysis of human cervical vertebral motion and head-neck-torso kinematics during low speed rear impacts. SAE Transactions, **106**: pp.3859–3876.

[15] Kang, YS., Millis, W. *et al.* (2021) Head-to-T1 relative rotation of the BioRID-II, Hybrid III, and post mortem human subjects with increased backsets in moderate-speed rear impacts. Proceedings of IRCOBI Conference, 2021, Beijing, China.

[16] Humanetics (2019) BioRID II Dummy Certification Manual [Rev. E], ARA-9901.

[17] Schneider, L. W., Robbins, D. H., Pflig, M. A. and Snyder, R. G. (1983) Development of Anthropometrically Based Design Specifications for an Advanced Adult Anthropomorphic Dummy Family, Volume 1.

[18] Kang, YS., Moorhouse, K. and Bolte, J. H. IV (2011) Measurement of six degrees of freedom head kinematics in impact conditions employing six accelerometers and three angular rate sensors (6aω configuration). J. Biomech. Eng., **133**(11): p. 111007.

[19] Kang, YS., Moorhouse, K., Herriott, R. G. and Bolte, J. H. IV (2009) A new instrumentation technique for the cervical spine of PMHS in rear impacts. Proceedings of IBS Conference, 2009, Columbus, Ohio, U.S.A.

[20] Slykhouse, L. *et al.* (2019) Anatomically-based skeletal coordinate systems for use with impact biomechanics data intended for anthropomorphic test device development. J. Biomech., **92**: pp.162–168.

[21] Kang, YS., Moorhouse, K. and Bolte, J. (2014) Head and cervical spine responses of post mortem human subjects in moderate speed rear impacts. Proceedings of IRCOBI Conference, 2014, Berlin Germany.

[22] SAE International (2022) Surface Vehicle Recommended Practice — Instrumentation for Impact Test Part 1: Electronic Instrumentation.

[23] Albery, C. and Whitestone, J. J. (2003) Comparison of cadaveric human head mass properties: mechanical measurement vs. calculation from medical imaging. Proceedings of Thirty-First International Workshop on Human Subjects for Biomechanical Research, 2003.

[24] Self, B. P., Spittle, E. K., Kaleps, I. and Albery, C. (1992) Accuracy and repeatability of the standard automated mass properties measurement system. Technical Report AL-TR-1992-0137, Armstrong Laboratory, Wright-Patterson AFB, Ohio.

[25] Kang, YS., Stammen, J., Moorhouse, K. and Bolte, J. (2016) PMHS lower neck load calculation using inverse dynamics with cervical spine kinematics and neck mass properties. Proceedings of IRCOBI Conference, 2016, Malaga, Spain.

[26] Di Domenico, L. and Nusholtz, G. (2003) Comparison of parametric and non-parametric methods for determining injury risk. SAE Technical Paper 2003-01-1362, 2003.

[27] Yoganandan, N., Stemper, B. D. and Rao, R. D. (2013) Patient mechanisms of injury in whiplash-associated disorders. Semin. Spine Surg., **25**(1): pp.67–74.

[28] Boström, O. et al. (1996) A new neck injury criterion candidate — based on injury findings in the cervical spinal ganglia after experimental neck extension trauma. Proceedings of IRCOBI Conference, 1996, Dublin, Ireland.

[29] Schmitt, K., Muser, M. H. and Niederer, P. (2001) A new neck injury criterion candidate for rear-end collisions taking into account shear forces and bending moments. Proceedings of International Technical Conference on the Enhanced Safety of Vehicles, 2001, Amsterdam, the Netherlands.

[30] Jin, F., Li, J., Liu, Z., Liu, B., Yang, Z. and Huang, J. (2025) Biomechanical rational for development of cervical kyphosis deformity: a finite element analysis. BMC Musculoskelet. Disord., **26**(1):p 1074.

[31] White, N. et al. (2009) Investigation of upper body and cervical spine kinematics of post mortem human subjects (PMHS) during low-speed, rear-end impacts. SAE Technical Paper 2009-01-0387, 2009.

[32] Van Ratingen, M., Ellway, J., Avery, M., Gloyns, P., Sandner, V., Versmissen, T. *et al.* (2009) The Euro NCAP Whiplash Test.

[33] Panjabi, M. M., Ito, S., Ivancic, P. C. and Rubin, W. (2005) Evaluation of the intervertebral neck injury criterion using simulated rear impacts. J. Biomech., **38**(8): pp.1694–1701.

[34] Kang, Y.-S. (2011) Evaluation of Biofidelity of Anthropomorphic Test Devices and Investigation of Cervical Spine Injury in Rear Impacts: Head-Neck Kinematics and Kinetics of Post Mortem Human Subjects. The Ohio State University.

[35] Brault, J. R., Siegmund, G. P. and Wheeler, J. B. (2000) Cervical muscle response during whiplash: evidence of a lengthening muscle contraction. Clin. Biomech., 15(6): pp.426–435.

[36] Siegmund, G. P., Sanderson, D. J., Myers, B. S. and Inglis, J. T. (2003) Awareness affects the response of human subjects exposed to a single whiplash-like perturbation. Spine (Phila. Pa. 1976)., 28(7): pp.671–679.

VIII. APPENDIX

Additional Whole-Neck Parameters

TABLE AI
Whole-Neck Parameters

	HTTRR (-) °	Force x (-) N	Force z (+) N	Moment y (+) Nm	# of Injuries
PMHS1	-27.6	-29	159	3.8	2
PMHS2	-19.1	-59	170	3.8	3
PMHS3	-11.1	-64	250	2.9	0
PMHS4	-0.1	-179	229	9.5	1
PMHS5	-12.6	-79	259	11.1	2
PMHS6	-30.5	-103	160	9.5	1

Normalisation Example

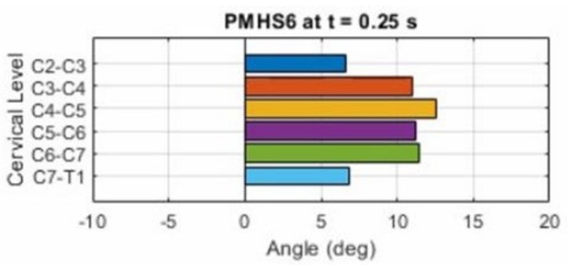

a) Recorded Intervertebral Rotation

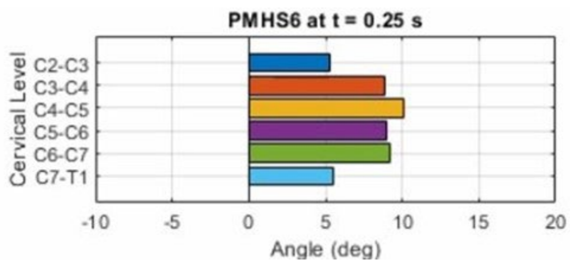

b) Intervertebral Rotation Normalised by PMHS

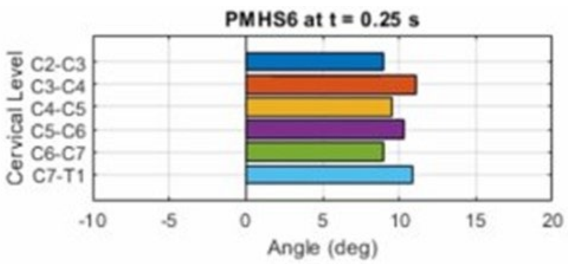

c) Intervertebral Rotation Normalised by Segment

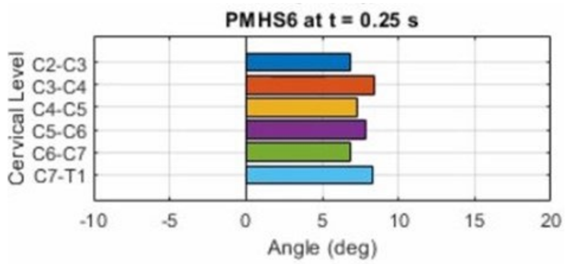

d) Intervertebral Rotation Normalised by Both

Fig. A1: Normalisation Procedure Example

Correlation

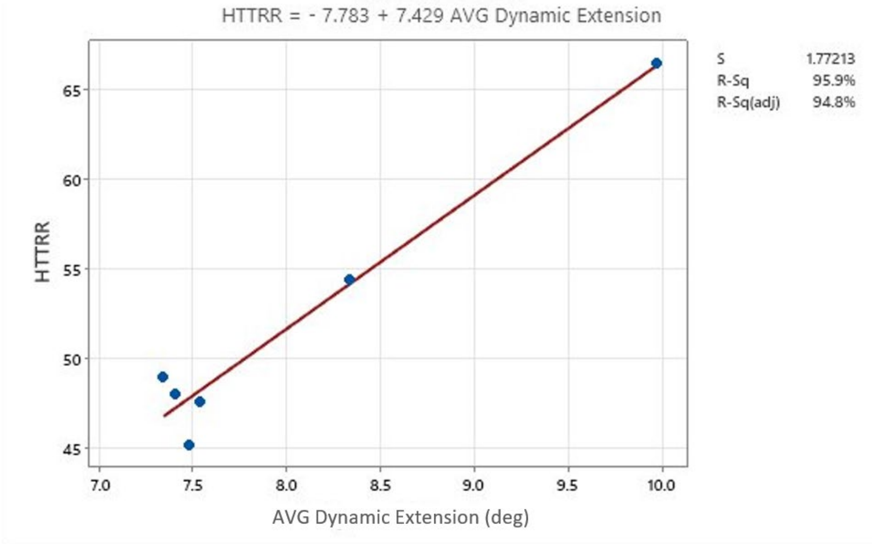

Fig. A2: HTTRR Correlation

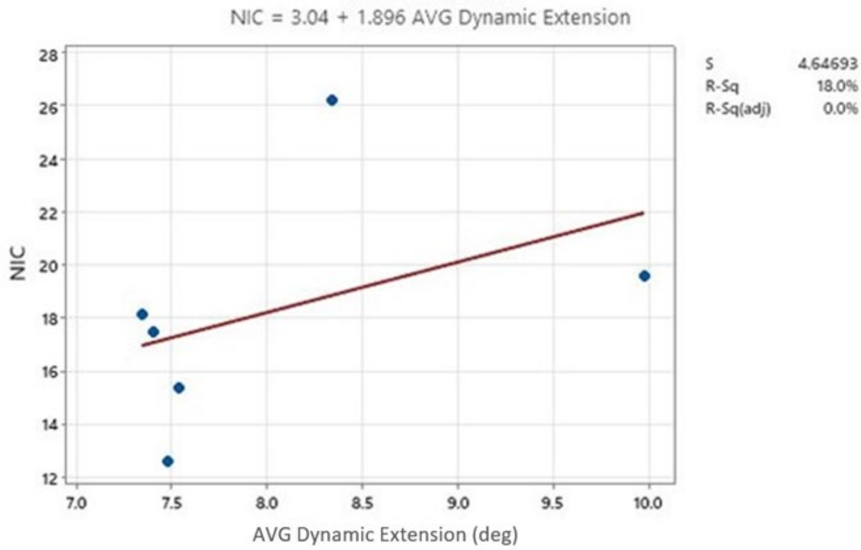

Fig. A3: NIC Correlation

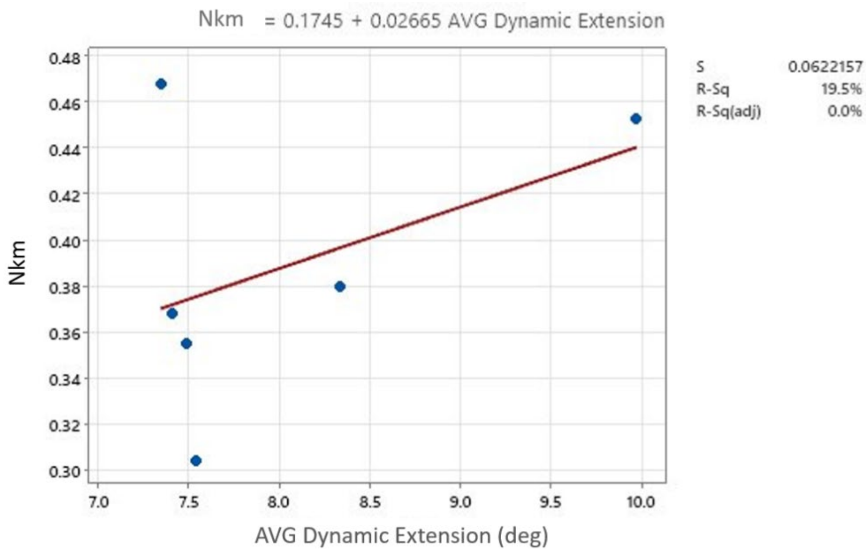

Fig. A4: Nkm Correlation

Time Histories for Injury Criteria

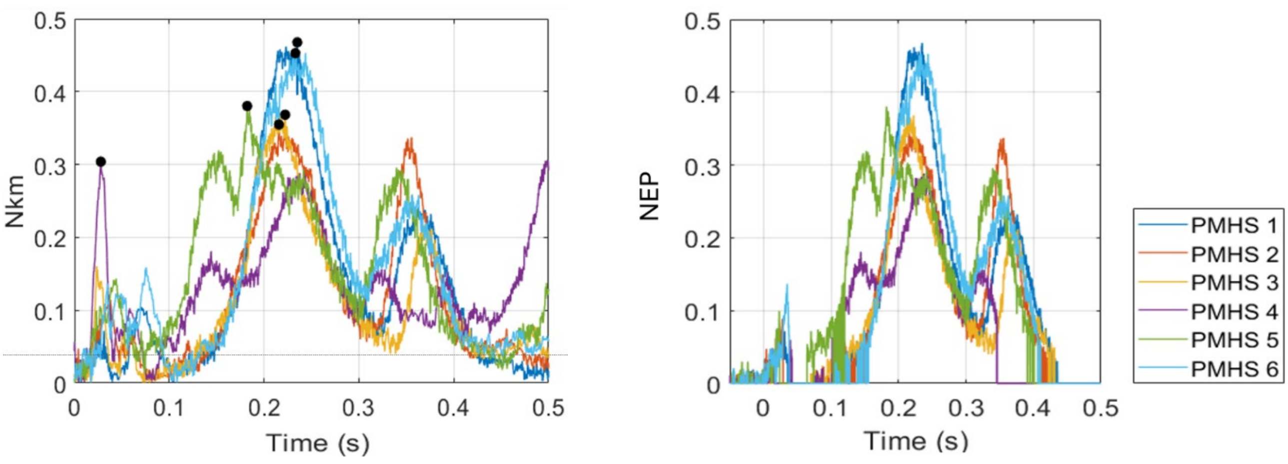

a) Nkm Components b) NEP

Fig. A5: Nkm Time History.

Black dots indicate maximum values. The NEP plot indicates when the polarity of the forces and moments are categorised as extension and positive shear, and the affiliated Nkm value during those windows.

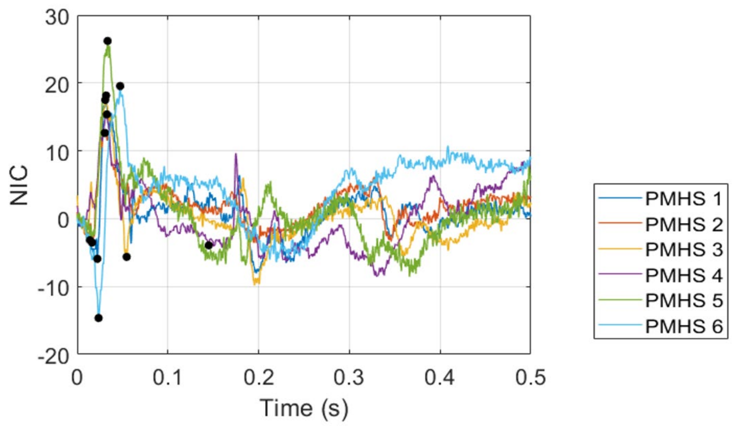

Fig. A6: NIC Time History.

Black dots indicate peak values in both the positive and negative extrema.